

Three-Dimensional Measurement and Cluster Analysis for Determining the Size Ranges of Chinese Temporomandibular Joint Replacement Prosthesis

Lu-Zhu Zhang, DDS, Shuai-Shuai Meng, MS, Dong-Mei He, DDS, MD, Yu-Zhuo Fu, PhD, Ting Liu, MS, Fei-Yu Wang, DDS, Min-Jun Dong, MS, and Yu-Si Chang, DDS

Abstract: The aim of this study was to investigate the osseous characteristics of Chinese temporomandibular joint (TMJ) and detect the size clusters for total joint prostheses design.

Computer tomography (CT) data from 448 Chinese adults (226 male and 222 female, aged from 20 to 83 years, mean age 39.3 years) with 896 normal TMJs were chosen from the Department of Radiology in the Shanghai 9th People's Hospital. Proplan CMF 1.4 software was used to reconstruct the skulls. Three-dimensional (3D) measurements of the TMJ fossa and condyle-ramus units with 13 parameters were performed. Size clusters for prostheses design were determined by hierarchical cluster analyses, nonhierarchical (K-means) cluster analysis, and discriminant analysis.

The glenoid fossa was grouped into 3 clusters, and the condyle-ramus units were grouped into 4 clusters. Discriminant analyses were capable of correctly classifying 97.24% of the glenoid fossa and 94.98% of the condyle-ramus units. The means and standard deviations for the parameter values in each cluster were determined.

Fossa depth and angles between the condyle and ramus were important parameters for Chinese TMJ prostheses design. 3D

measurements and cluster analysis of the osseous morphology of the TMJ provided an anatomical reference and identified the dimensions of the minimum numbers of prosthesis sizes required for Chinese TMJ replacement.

(*Medicine* 95(8):e2897)

Abbreviations: CT = computer tomography, 3D = three-dimensional, PCA = principal component analysis, TMJ = temporomandibular joint.

INTRODUCTION

The temporomandibular joint (TMJ) is an atypical diarthrodial synovial joint that is capable of performing both the translational and rotational movements of the mandible. The TMJ is formed by the mandibular condyle and glenoid fossa of the squamous part of the temporal bone and is separated into upper and lower cavities by the presence of an articular fibrocartilaginous disc.¹ End-stage TMJ pathologies require resection and replacement of the joint to restore the normal TMJ anatomy and function.² It is important that any prosthetic device has the correct dimensions and angles to fit its intended site. However, the standard prosthesis in the market (Biomet/Lorenz, Warsaw, IN) was designed with flat fossa bone contact plane that was suitable for most Caucasians with shallow fossa structure.^{3,4} Studies have shown that the percentage of very concave fossa is 19% among Chinese and 4% in Caucasians.^{5,6} The mean fossa depth of Chinese is 0.68 mm (118 cases and 236 sides); however, there are no reports of fossa depth in Caucasians. These differences could lead to problems, such as prosthesis mismatches, increased bone trimming times, and the risk of skull base injury during the operation.⁷ In order to develop a set of TMJ prostheses that is suitable Chinese patients, the anatomical features of Chinese TMJs should be studied.

Currently, our understanding of the anatomical features of the TMJ has come primarily from direct caliper measurements of a limited number of dry skull specimens. The lack of cartilage covering of the TMJ can cause measurement deviations. Moreover, the medical histories of TMJ disease of those dry skull specimens are still missing. Some key measurements, including the anterior and posterior inclination angles between the condyle and ramus, which are critical for the design of TMJ prostheses have not been reported. The emergence of computer-aided design has provided a new method for accurate measurements. With three-dimensional (3D) reconstructions of the skull based on computer tomography (CT) scans, anatomical landmarks can be defined, and distances and angles between those landmarks can be measured. In this manner, the number of samples can be greatly enlarged to the range of all patients, and their medical histories can be easily traced as a reference for the selection of a normal TMJ.

Editor: Giancarlo Carli.

Received: October 3, 2015; revised: January 12, 2016; accepted: January 29, 2016.

From the Department of Oral Surgery, College of Stomatology (L-ZZ, D-MH, F-YW, Y-SC); Department of Radiology (M-JD); Ninth People's Hospital, Shanghai Jiao Tong University School of Medicine; and Department of Micro-Nano Electronics, School of Electronic Information and Electrical Engineering, Shanghai Jiao Tong University, Shanghai, China (S-SM, Y-ZF, TL).

Correspondence: Dong-Mei He, Department of Oral Surgery, College of Stomatology, Ninth People's Hospital, Shanghai Jiao Tong University School of Medicine, 639 Zhi Zao Ju Road, Huangpu District, Shanghai 200011, China (e-mail: lucyhe119@163.com); Yu-Zhuo Fu, Department of Micro-Nano Electronics, School of Electronic Information and Electrical Engineering, Shanghai Jiao Tong University, 800 Dongchuan Road, Minhang District, Shanghai 200240, China (e-mail: yzfu@sjtu.edu.cn); Min-Jun Dong, Department of Radiology, School of Medicine, Ninth People's Hospital, Shanghai Jiao Tong University School of Medicine, 639 Zhi Zao Ju Road, Huangpu District, Shanghai 200011, China (e-mail: peter_dongmj@yeah.net).

Z-LZ, S-SM, TL and F-YW contributed equally to this work.

This study was supported by grants from the National Natural Science Foundation of China (81472117), the Fund of Medicine and Engineering Interdisciplinary Research of Shanghai Jiao Tong University (YG2014MS05), and the Science and Technology Commission of Shanghai Municipality Science Research Project (14DZ2294300), Ninth college students innovation training project of Shanghai Jiao Tong University School of Medicine (2015502).

The authors have no conflicts of interest to disclose.

Copyright © 2016 Wolters Kluwer Health, Inc. All rights reserved. This is an open access article distributed under the Creative Commons Attribution-NonCommercial-NoDerivatives License 4.0, where it is permissible to download, share and reproduce the work in any medium, provided it is properly cited. The work cannot be changed in any way or used commercially.

ISSN: 0025-7974

DOI: 10.1097/MD.0000000000002897

In this study, a 3D TMJ measurement method for prosthesis design was established. CT data from adult normal TMJs were collected, measured, and analyzed by cluster analysis to provide a reference for prosthesis design for the Chinese population.

MATERIALS AND METHODS

Study Population

This is a retrospective study, which involved anonymous human skull CT data. This study was approved by the local ethics board of the hospital (Scientific Research Projects Approval Determination of Independent Ethics Committee of Shanghai Ninth People's Hospital affiliated to Shanghai Jiao-Tong University, School of Medicine, 2014-46). A total of 448 adult patients (over 20 years old) diagnosed of normal TMJ (bone morphology of the TMJ fossa and condyle are smooth without fracture, neoplasia, resorption, and hyperplasia) based on CT scans were recruited from the database of the Department of Radiology of the Shanghai Ninth People's Hospital. Patients who had condylar or zygomatic root fracture, condylar bone cyst, TMJ degenerative disease like osteoarthritis or condylar resorption, tumor or condylar hyperplasia, etc. were excluded. There were 226 females and 222 males, and the ages ranged from 20 to 83 years old (mean 39, standard deviation 12.44). All patients have been conducted according to the principles expressed in the Declaration of Helsinki when they took CT scan examination. Because the data were analyzed anonymously, no consent was given. All CT data were acquired

using Philips Brilliance 64-slice CT scanner (Philips Medical Systems Inc., Cleveland, OH). The CT scanning parameters were the field of CT scan was from the chin to the eyebrow including the maxillofacial region and mandible. It was a helical CT volume scan with a matrix of 512×512 . The slice thickness is 1 mm. The data were stored and imported into the ProPlan CMF 1.4 software (Materialise NV) for 3D cranial-maxillofacial reconstruction. A specific CT range (2950–2976 Hounsfield units) as bone demonstration was used for measurement. This software is generally used for interactive virtual surgery planning, simulation, and the output of patient-specific surgical guides to transfer the plan to the operating room. It was especially developed for processing CT data for accurately and predictably planning cranio-maxillofacial surgeries including visualize the patient anatomy and measurement. It is a widely used software now.⁷ We also measured several dry skull specimens' TMJ by caliper and compared the data with the 1 measured from CT scan by Proplan CMF 1.4 software. The 2 measurements have significant correlation (ICC = 0.99). In order to reduce the interexaminer error, we had 2 examiners measured the data separately. Their measurement reliability was evaluated by intraclass correlation coefficient (ICC), which was 0.94. Each examiner measured the parameters 3 times and calculated the mean value as the final results to reduce the intraexaminer error.

Measurements and Statistical Analysis

The CT data of the patients were imported into the ProPlan CMF 1.4 software (Materialise, Leuven, Belgium) for 3D skull

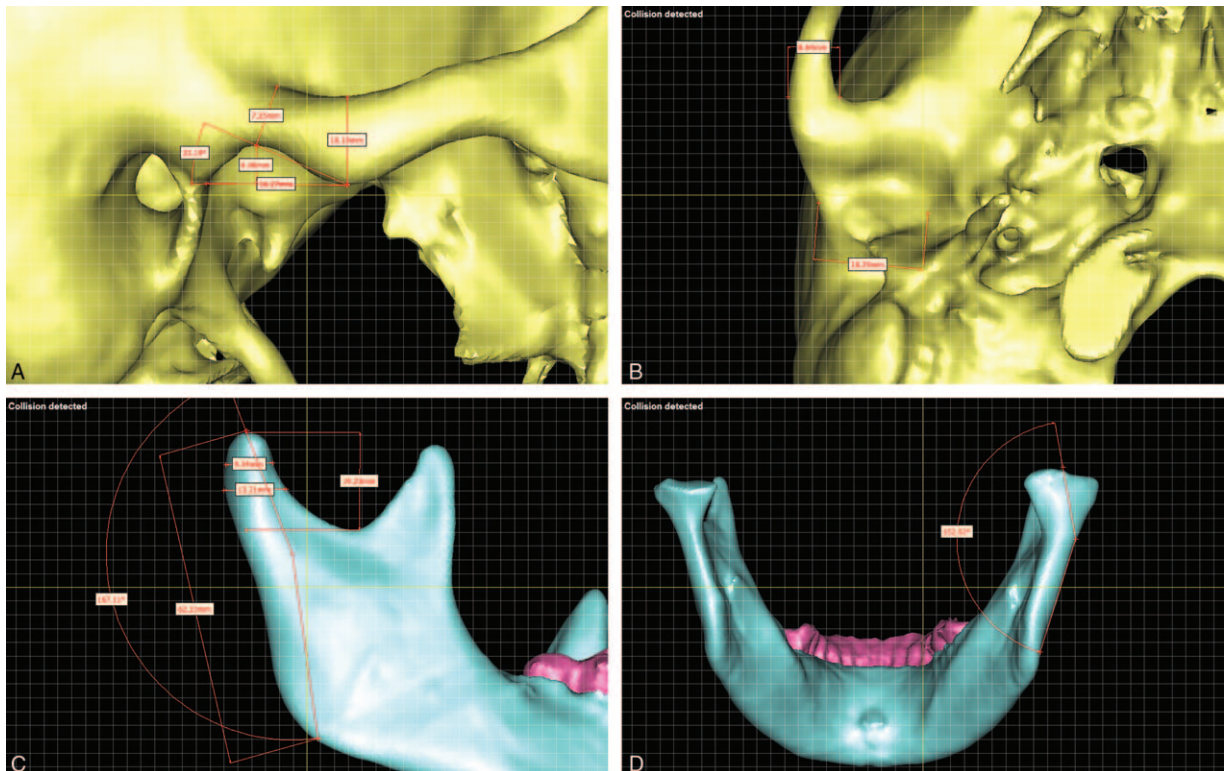


FIGURE 1. Temporomandibular joint (TMJ) measurements. (A) Fossa length, depth, anterior slope angle, height of the articular eminence, and width of the zygomatic root. (B) Interior and exterior diameters of the glenoid fossa and thickness of the zygomatic root. (C) Posterior inclination angle of the condyle-ramus unit, ramus length, anteroposterior diameters of the condylar head and neck, height of the condylar head. (D) Interior inclination angle of the condyle-ramus unit.

TABLE 1. 3D-Measurement of Temporomandibular Joint Morphology

Fossa	The lateral depth of glenoid fossa, mm	D1
	The anterior slope angle of glenoid fossa, °	A1
	The anteroposterior diameter of glenoid fossa, mm	D2
	The interior and exterior diameter of glenoid fossa, mm	D3
	The height of articular eminence, mm	H1
	The width of zygomatic root, mm	W1
Condyle-ramus unit	The thickness of zygomatic root, mm	T1
	The posterior inclination angle of condyle, °	A2
	The interior inclination angle of condyle, °	A3
	The length of ramus, mm	L1
	The anteroposterior diameter of condylar head, mm	D4
	The anteroposterior diameter of condylar neck, mm	D5
	The height of condylar head, mm	H2

reconstruction. Thirteen measurement parameters including depth of the glenoid fossa, angles between the condyle, and ramus which were highly related with the prosthesis design were selected to describe the morphologies of the TMJ fossa (Figure 1A, B) and condyle-ramus unit (Figure 1C, D; Table 1). The distribution of the lateral depths of the glenoid fossa were grouped as 3 categories: flatten (≤ 3 mm), shallow (3–4.5 mm), and deep (> 4.5 mm). The average value of each parameter were recorded and compared between the males and females using the Statistical Package for the Social Sciences software package, version 13.0 (SPSS, Chicago, IL) and the Student's *t*-test. An α level of ≤ 0.05 was considered significant.

Cluster Analysis

Clustering analysis is one of the most effective tools in data mining and was used to group the sample of TMJs into “clusters” according to their measurements. Each cluster represented a specific TMJ shape, and the samples within the same cluster exhibited the maximum similarity across multiple measurement features. For the measurement parameters shown in Table 1, the value of each parameter could have a different variance and comparable scales. Moreover, there will be correlations between the measurement datasets. For example, the depth of the glenoid fossa (D1) and the anterior slope angle of glenoid fossa (A1) are very important for fossa prosthesis design; therefore, prior to the cluster analysis, we applied pretreatment techniques of Z-scoring⁸ and principal component analysis (PCA) to normalize the original measurement results and reconstruct data into an orthonormal system of Euclidean space. PCA is a multivariate analysis method that has been widely used in the analysis of large multidimensional datasets. After PCA processing, the scale of the dataset can be reduced by retaining only the measurement characteristics that contribute the most to the variance.⁹ Because different measurements may be more or less important to TMJ replacement design, we set weights for each of the TMJ measurements to constrain their influences on the cluster analysis.

In this study, hierarchical cluster analysis was performed to determine the number of clusters required for final classification. In the process of agglomerative hierarchical clustering, each

sample is initialized as a cluster and then samples in different clusters gradually merge to form larger clusters. The process continues until all of the samples are in the same cluster or a prespecified termination condition is reached.¹⁰ The predefined distance value is the metric that is used to determine which clusters are closest to each other. In this study, we used the average distance to measure the distances between clusters. We utilized the “similarity level” metric to evaluate the results of the hierarchical cluster analysis. The relationship between the “similarity level” and the number of clusters is used to indicate the optimal number of clusters for a specific scenario.

After the optimal number of clusters was determined, we performed K-means clustering to identify the cluster centers and construct an average model for each shape. The K-means algorithm first randomly selected *k* data objects and initializes each data object as the center of a cluster. The remaining data objects are allocated to the nearest cluster according to their distances from the cluster centers. The average center of a cluster is recalculated each time a new object joins that cluster.¹¹ In the present paper, we chose the *k* samples that resulted in the greatest average distances between clusters as the initial cluster centers. This fixed initial cluster centers method is able to provide global convergence and to overcome local optima.

Discriminant Analysis

Discriminant analysis is a multivariate statistical method that can distinguish newly acquired samples according to the quantitative characteristics of an existing set of observed samples.¹² In the present paper, we utilized discriminant analysis to determine how well the clustering analysis was able to classify the TMJs based on shape. One important metric for evaluating such classification results is the proportion correct.¹³ In the present study, when a sample TMJ object in 1 cluster was closer to the center of its own cluster than the center of any other cluster, that sample was deemed to be correctly classified. The “proportion correct” value can be calculated in the form of the percentage C/S where C is the number of TMJ samples that have been correctly classified, and S is the total number of TMJ samples.

RESULTS

Statistical Comparisons of the Measurements Between the Female and Male TMJs

Table 2 shows the measurements for the glenoid fossae, zygomatic arches, and articular eminences. There were no significant differences between the right and left side of the above parameters. Whereas there were significant differences between males and females.

Table 3 shows the measurements of the condyles and ramus units. There were no significant differences between the right and left side of the mandible. Whereas there were significant differences between males and females.

Table 4 shows the distribution of the lateral depths of the glenoid fossae. Although there were significant difference between the males and females, flatten fossa accounted very low percentage of them, whereas nearly 1/3 males and 1/2 females had deep fossa.

Cluster Analysis of Chinese TMJs

Generally, in the process of PCA, the reduction of the dimensionality of a dataset improves the effectiveness of

TABLE 2. Measurement Results of Glenoid Fossa, Zygomatic Arch, and Articular Eminence

Measurements	Average	Male Average	Female Average	P Value
Lateral depth of glenoid fossa, mm	4.32 ± 1.03	4.56 ± 1.01	4.07 ± 0.98	0.00
Anterior slope angle of glenoid fossa, °	25.61 ± 5.39	27.01 ± 5.39	24.16 ± 4.99	0.00
Anteroposterior diameter of glenoid fossa, mm	15.05 ± 1.79	14.72 ± 1.69	15.39 ± 1.82	0.00
Interior and exterior diameter of glenoid fossa, mm	22.03 ± 2.08	22.68 ± 1.92	21.36 ± 2.03	0.00
Height of articular eminence, mm	9.69 ± 1.34	10.09 ± 1.29	9.28 ± 1.27	0.00
Width of zygoma root, mm	5.73 ± 1.64	5.58 ± 1.27	5.87 ± 1.24	0.001
Thickness of zygoma root, mm	5.26 ± 0.83	5.50 ± 0.84	5.01 ± 0.74	0.00

subsequent clustering analyses and simultaneously introduces data feature loss. In this study, the original measurement dimensions of the fossa and condyle were 7 and 6, respectively, as indicated in Table 1. Taking the data characteristics of the dataset without dimension reduction as 100%, we utilized the variances of the retained data to evaluate the data characteristic retention rate when the data dimensions of the fossa and condyle were reduced to 5, 4, and 3. For the fossa, the results revealed that the retained data characteristics were 97.21%, 94.52%, and 90.91% when the fossa dimensions were reduced to 5, 4, and 3, respectively. For the condyle, the corresponding results were 99.40%, 97.62%, and 94.86%. We can see that the data characteristic loss was not linear with respect to dimension reduction. Even in the 3-dimension scenario, that is, when the mean number of measurement dimensions had been reduced by half or more for both the fossa and condyle, more than 90% of the data characteristics were retained. Thus, we exploited PCA to greatly reduce the computational complexity of the later clustering procedure at a very small cost of data characteristics loss.

After the PCA process, all of the measurements of the TMJ were projected into 4 scenarios (i.e., no dimensional reduction, 5 dimensions, 4 dimensions, and 3 dimensions) and were ready for the hierarchical cluster analysis. Figures 2 and 3 plot the similarity level against the number of clusters from the hierarchical cluster analysis for each scenario. Figure 2A describes the results of the original 7-dimensional fossa dataset without any reduction. We can see the similarity level dropped sharply when the number of clusters was reduced to 4, which indicates that the optimal number of clusters was 4 in this scenario. Similarly, Figure 2B to D illustrates that when the dimensions were reduced from 7 to 5, 4, and 3, the optimal numbers of clusters were 3, 4, and 3, respectively. Similarly, Figure 3 indicates that the optimal numbers of clusters for the condyle were 3, 4, 4, and 4 when the dataset dimensions were 6 (original), 5, 4, and 3, respectively.

TABLE 3. Measurement Results of the Condyle and Ramus

Measurements	Average	Male Average	Female Average	P Value
Posterior inclination angle of condyle, °	160.10 ± 5.02	160.45 ± 4.92	159.73 ± 5.10	0.044
Interior inclination angle of condyle, °	151.34 ± 5.69	150.93 ± 5.97	151.77 ± 5.35	0.035
Ramus length, mm	58.72 ± 5.78	61.66 ± 5.08	55.70 ± 4.81	0.00
Anteroposterior diameter of condylar head, mm	11.23 ± 1.36	11.49 ± 1.40	10.97 ± 1.28	0.00
Anteroposterior diameter of condyle neck, mm	12.02 ± 1.25	12.33 ± 1.15	11.71 ± 3.25	0.00
Height of condyle head, mm	16.14 ± 3.12	16.37 ± 3.25	15.90 ± 2.97	0.034
Posterior inclination angle of condyle, °	160.10 ± 5.02	160.45 ± 4.92	159.73 ± 5.10	0.044
Interior inclination angle of condyle, °	151.34 ± 5.69	150.93 ± 5.97	151.77 ± 5.35	0.035

TABLE 4. Classification of Temporomandibular Joint (TMJ) Glenoid Fossa

Glenoid Fossa Type	Male, %	Female, %	P Value
Flatten (<3 mm)	13.01	3.95	0.00
Shallow concaved (3–4.5 mm)	52.83	44.94	0.00
Deep concaved (>4.5 mm)	33.16	51.11	0.00

Using the optimal numbers of clusters derived in the previous step, we applied K-means clustering analyses to all 4 of the scenarios. Here, we utilized the discriminant analysis method to calculate the proportion correct for the results of each scenario. Higher proportion correct values indicate better clustering results. In the 4 scenarios, the proportion correct values for the fossa were 94.98%, 96.61%, 94.60%, and 97.24%. For condyle, the corresponding results were 94.35%, 94.48%, 94.35%, and 94.98%.

We can see that the 3-dimension scenario achieved the highest correctness scores for both the fossa and condyle, which indicated that this configuration achieved the optimal categorization of the current observations. In the 3-dimension scenario, the corresponding optimal cluster numbers derived from the K-means clustering analysis indicated that there were 3 fossa types and 4 condyle types, which are shown in Figures 2D and 3D. We adopted the measurements at the centers of each cluster to construct an “average model” for each fossa and condyle type. The detailed results are shown in Tables 5 and 6.

DISCUSSION

Because the delicate anatomical structure of the TMJ accounts for its movable features, the normal and affected

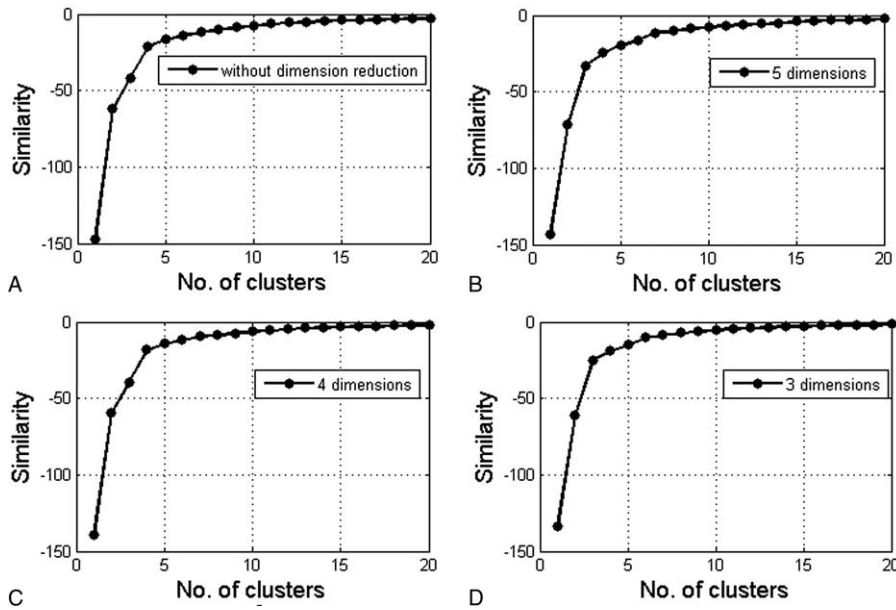


FIGURE 2. The similarity level plotted against the number of clusters after hierarchical analysis of the fossa. (A) Without dimension reduction; (B) 5 dimension; (C) 4 dimension; and (D) 3 dimension.

osseous structures of the TMJ are crucial for understanding its physiological properties and the development of TMJ diseases. Öberg et al¹⁴ first contributed to our knowledge of the osseous structure of the TMJ by suggesting a systemic measuring method and conducting measurements on patients who were categorized by age. With the acquired measurements, he described the osseous structural differences between the normal and affected TMJs of full dentition, partial anodontia, and edentulous patients and concluded that osseous structural changes caused by osteoarthritis are most likely found around condylar head or the

middle-exterior 1/3 of the glenoid fossa. Subsequently to Öberg, the osseous structure of TMJ and the corresponding occlusion features were further explored by Hinton¹⁵ and Mongini¹⁶ using a similar method. In China, similar studies were performed by Xu et al^{5,6} on dry skull specimen. In his study, Xu defined landmarks for measurements, revealed the anatomical features of the TMJs of Chinese people, established a classification method for different TMJs, and reported the anatomical differences between Chinese people and Caucasians. Similar conclusions were also reported by Yao et al¹⁷ based on measurements of 30 dry skull

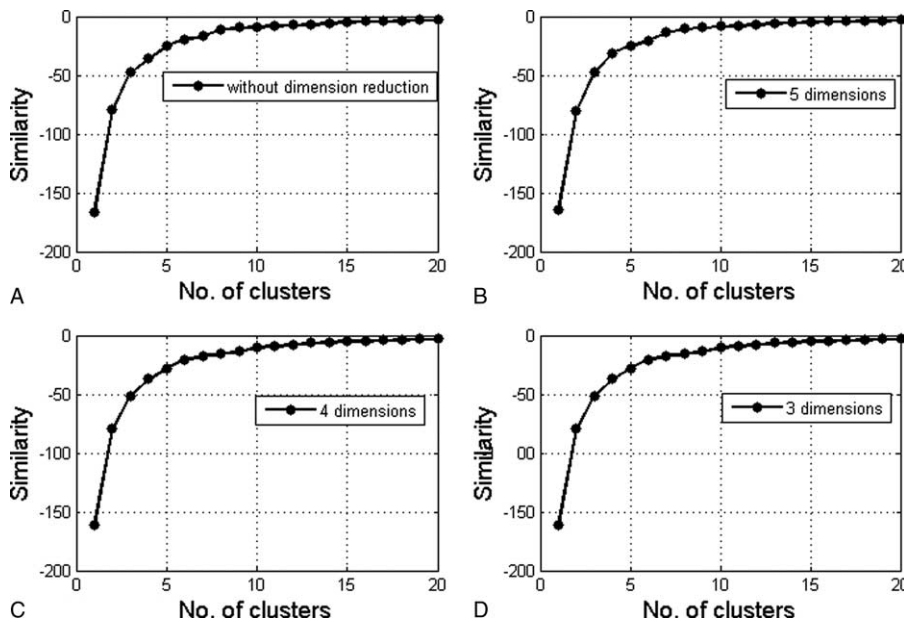


FIGURE 3. The similarity level plotted against the number of clusters after hierarchical analysis of the condyle-ramus unit. (A) Without dimension reduction; (B) 5 dimension; (C) 4 dimension; and (D) 3 dimension.

TABLE 5. The 3 Clusters of Fossa Measurements From the K-Means Clustering Analysis

Cluster No.	No. of Samples	D1, mm	A1, °	L1, mm	D2, mm	H1, mm	W1, mm	T1, mm
1	255	3.21	20.36	14.53	21.54	9.05	6.23	5.11
2	354	4.40	26.21	15.15	22.02	9.68	5.61	5.26
3	188	5.68	31.59	15.58	22.71	10.60	5.25	5.46

specimen using the same method. However, those studies were based on a limited number of dry skull specimens, and the researchers were unable to judge the health conditions of the TMJs due to the lack of medical histories and image diagnostics.

In contrast, CT and magnetic resonance imaging (MRI) imaging technologies have been rapidly developed and widely used for evaluations and diagnoses of TMJs. Because MRI can accurately reflect soft tissue structures, Matsumoto et al¹⁸ performed osseous measurements of the glenoid fossa and condyles with the aid of coronal MRI and then divided the sample into 3 categories, that is, flat, horned, and concave. Also based on an MRI study, Ohnuki et al¹⁹ described the inter-relationship of positional and morphological changes in the articular disc with osseous changes in the TMJ and provided a foundation for treatment evaluation. Moreover, Geiger et al²⁰ further demonstrated the feasibility of TMJ measurement by analyzing and comparing the results of TMJ measurements from MRI, CT, and merged MRI and CT images. Although Matsumoto et al¹⁸ and Ohnuki et al¹⁹ measured patients with available medical histories, their measurements were primarily taken from 2-dimensional (2D) images along the direction of the scan, which resulted in a lack of generality and knowledge regarding the osseous structure of the TMJ in all 3 dimensions. Therefore, in the present study, we performed 3D measurements on 3D skull models that were reconstructed from medical images. We also proposed several measurements that are highly relevant to prosthesis design but have not yet been reported, such as the depth and diameter of the fossa and the posterior and interior inclination angles of the condyle-ramus unit.

Apart from custom devices that are suited to individual TMJ fossa, other options are limited. The Biomet stock device has a flat bone contact plane that requires bone trimming for device positioning. Deeper fossa depths require more bone trimming, which could increase the risk of skull base perforation. In the present study, we found that the mean fossa depth among the Chinese population is 4.32 mm. Although there were no significant differences between the right side and left side of the fossa, deep fossa depth was accounted for 33.16% in males and 51.11% in females, which had significantly difference. This information is very important for the design and fixation of fossa prostheses. Regarding standard prostheses such as the Biomet total joint replacement system, the fossa prostheses are in flat contact with the bone, which means that bone trimming of

the fossa is necessary for prosthesis positioning. Deeper fossae require more bone trimming, which could increase the risk of skull base injury, especially among the Chinese population, which was found to have a high percentage of deep fossa in the present study. The other very important measurement in this study is the angle between the condyle and ramus. The 2 angles that could affect ramus prosthesis positioning with standard prostheses are the posterior inclination angle and the interior inclination angle. Although there were no significant differences between the right and left side of the mandible, in this study, cluster analysis revealed 4 types of condyle-ramus unit characteristics, whereas there is only 1 type of standard ramus prosthesis on the market, which could cause problems such as the lateral dislocation of the prosthesis out of the fossa or anterior dislocation that could injury the inferior alveolar nerve. Therefore, additional types of fossa and ramus prostheses may be needed to accommodate a wider variety of patients.

The most significant contribution of this study is that we applied a complete series of data-mining techniques, including data preparation, hierarchical cluster analysis, K-means analysis, and discriminant analysis, to identify the most reasonable measurements for Chinese TMJ replacement prosthesis sizing. In the data preparation procedure, we applied Z-scoring and PCA to enable the projection of all of the observed measurements into an orthonormal system of Euclidean space with comparable scales and appropriate dimensions. Next, hierarchical clustering analysis and K-means clustering techniques were applied to derive the optimal numbers and center point measurements of the clusters. Finally, the discriminant analysis was utilized to evaluate the correctness of the clustering analysis results.

In the process of PCA, hierarchical clustering analysis, and K-means clustering, we adjusted the weights of each TMJ measurement as an “impact factor” according to its anatomical and biological importance. For example, the lateral depth of the glenoid fossa (D1) is believed to be more significant than the thickness of the zygoma root (T1), so the weight of D1 was greater than that of T1. In the present study, the weights of the fossa measurements D1, A1, D2, D3, H1, W1, and T1 were set to 30%, 19%, 15%, 15%, 7%, 7%, and 7%, respectively, and weights of the condyle measurements A2, A3, L1, D4, D5, and H2 were set to 25%, 25%, 25%, 9%, 9%, and 7%, respectively. Consequently, each measurement had a different level of influence on the subsequent clustering procedures according to its degree of importance.

TABLE 6. The 4 Clusters of Condyle-Ramus Unit Measurements From the K-Means Clustering Analysis

Cluster No.	No. of Samples	A2, °	A3, °	L1, mm	D4, mm	D5, mm	H2, mm
1	192	154.82	152.14	61.57	11.77	12.74	16.86
2	134	159.11	143.09	57.68	11.12	11.94	15.42
3	240	160.68	155.04	52.95	10.69	11.31	15.06
4	231	164.44	151.62	62.97	11.42	12.21	17.08

Tables 5 and 6 illustrate the final results of our clustering analysis. Each cluster represents a distinct shape that was derived from the measurements of nondegenerative TMJs in our database. We referred to the center point values of each of the clusters as the average models for each TMJ type. We can see all of the measurements of the fossae varied significantly between types 1, 2, and 3 in Table 5. For each of the fossa types, the sample numbers ranged from 188 to 354. In contrast to the fossa types, the value of the condyle measurement A3 was quite similar for condyle types 1 and type 4 as shown in Table 6. Moreover, the condyle measurement A2 for condyle type 4 was much larger than those of the other condyle types. The numbers of condyle samples in each type ranged from 134 to 240. There were no extremely common or extremely rare fossa or condyle types, which indicate that the data preparations resulted in a credible distribution.

Furthermore, the above results could help each individual patient find the best-fitting prosthesis through procedures similar to those described in this paper. Until that goal is achieved, the addition of more measurement samples to the database will enable the data mining algorithms to “learn” from the new information and regenerate smarter clustering sets. Therefore, the cluster values in Tables 5 and 6 may be refined as more samples become available.

In conclusion, a 3D TMJ measurement method was established in this study. We identified 3 fossa types and 4 condyle-ramus unit types based on main parameters of fossa depth and angles of condyle-ramus angles by cluster analysis and thus provided a reference for total joint prosthesis design for the Chinese population.

ACKNOWLEDGMENTS

The authors thank Dr Guo Bai, and Yi Li's contributions to the measurement of part of the cases in this study. The authors also thank grants from the National Natural Science Foundation of China (81472117), the Fund of Medicine and Engineering Interdisciplinary Research of Shanghai Jiao Tong University (YG2014MS05), and the Science and Technology Commission of Shanghai Municipality Science Research Project (14DZ2294300), and Ninth college students innovation training project of Shanghai Jiao Tong University School of Medicine (2015502).

REFERENCES

1. Mercuri LG, Edibam NR, Giobbie-Hurder A. Fourteen-year follow-up of a patient-fitted total temporomandibular joint reconstruction system. *J Oral Maxillofac Surg.* 2007;65:1140–1148.
2. Wolford LM, Mercuri LG, Schneiderman ED, et al. Twenty-year follow-up study on a patient-fitted temporomandibular joint prosthesis: the Techmedica/TMJ Concepts device. *J Oral Maxillofac Surg.* 2015;73:952–960.
3. Granquist EJ, Quinn PD. Total reconstruction of the temporomandibular joint with a stock prosthesis. *Atlas Oral Maxillofac Surg Clin North Am.* 2011;19:221–232.
4. Leandro LF, Ono HY, Loureiro CC, et al. A ten-year experience and follow-up of three hundred patients fitted with the Biomet/Lorenz Microfixation TMJ replacement system. *Int J Oral Maxillofac Surg.* 2013;42:1007–1013.
5. Xu X, Feng G, Zhang J, et al. Osseous morphology of the temporomandibular joint. *Chin J Anat.* 1986;9:38–41.
6. Xu X, Wu J, Zhang J, et al. Measurement and analysis of the osseous part of the temporomandibular joint. *Acta Anat Sin.* 1986;17:343–347.
7. Bai G, He D, Yang C, et al. Application of Digital Templates to Guide Total Alloplastic Joint Replacement Surgery with Biomet Standard Replacement System. *J Oral Maxillofac Surg.* 2014;72:2440–2452.
8. Wang ML, Yao H, Xu WB. Prediction by support vector machines and analysis by Z-score of poly-l-proline type II conformation based on local sequence. *Comput Biol Chem.* 2005;29:95–100.
9. Nejadgholi I, Bolic M. A comparative study of PCA, SIMCA and Cole model for classification of bioimpedance spectroscopy measurements. *Comput Biol Med.* 2015;63:42–51.
10. Leski JM, Kotas M. Hierarchical clustering with planar segments as prototypes. *Pat Recog Lett.* 2015;54:1–10.
11. Al-Mohair HK, Saleh JM, Suandi SA. Hybrid human skin detection using neural network and K-means clustering technique. *Appl Soft Comput.* 2015;33:337–347.
12. Lei D, Holder RL, Smith FW, et al. Cluster analysis as a method for determining size ranges for spinal implants: disc lumbar replacement prosthesis dimensions from magnetic resonance images. *Spine.* 2006;31:2979–2983.
13. Zhou S, Xu Z, Tang X. Method for determining optimal number of clusters in K-means clustering algorithm. *J Comput Appl.* 2010;30:1995–1998.
14. Öberg T, Carlsson GE, Fajers CM. The temporomandibular joint. A morphologic study on a human autopsy material. *Acta Odontol Scand.* 1971;29:349–384.
15. Hinton RJ. Relationships between mandibular joint size and craniofacial size in human groups. *Arch Oral Biol.* 1983;28:37–43.
16. Mongini F. Anatomic and clinical evaluation of the relationship between the temporomandibular joint and occlusion. *J Prosthet Dent.* 1977;38:539–551.
17. Yao XD, Fan SQ, An G, et al. The measurements and analysis of temporomandibular joint bony structures. *J Pract Stomatol.* 2011;27:801–804.
18. Matsumoto K, Kameoka S, Amemiya T, et al. Discrepancy of coronal morphology between mandibular condyle and fossa is related to pathogenesis of anterior disk displacement of the temporomandibular joint. *Oral Surg Oral Med Oral Pathol Oral Radiol.* 2013;116:626–632.
19. Ohnuki T, Fukuda M, Nakata A, et al. Evaluation of the position, mobility, and morphology of the disc by MRI before and after four different treatments for temporomandibular joint disorders. *Dento-maxillofac Radiol.* 2006;35:103–109.
20. Geiger D, Bae WC, Statum S, et al. Quantitative 3D ultrashort time-to-echo (UTE) MRI and micro-CT ((CT) evaluation of the temporomandibular joint (TMJ) condylar morphology. *Skeletal Radiol.* 2014;43:19–25.